

Atmospheric Chemistry of HFC-236cb: Spectrokinetic Investigation of the CF₃CF₂CFHO₂ Radical, Its Reaction with NO and NO₂, and the Fate of the CF₃CF₂CFHO Radical

Trine E. Møgelberg, Anders Feilberg,[†] Anders M. B. Giessing,[†] Jens Sehested, and Merete Bilde

Section for Chemical Reactivity, Environmental Science and Technology Department, Risø National Laboratory, DK-4000 Roskilde, Denmark

Timothy J. Wallington*

Ford Research Laboratory, SRL-E3083, Ford Motor Company, P. O. Box 2053, Dearborn, Michigan 48121-2053

Ole J. Nielsen*

Ford Motor Company, Ford Forschungszentrum Aachen, Dennewartstrasse 25, D-52068 Aachen, Germany

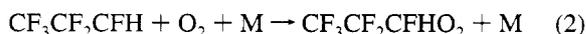
Received: June 23, 1995; In Final Form: August 18, 1995[®]

A pulse radiolysis technique was used to study the UV absorption spectrum of CF₃CF₂CFHO₂ radicals (at 250 nm $\sigma = (175 \pm 36) \times 10^{-20}$ cm² molecule⁻¹). The observed bimolecular rate constant for the self reaction of CF₃CF₂CFHO₂ radicals was $k_{1,obs} = (5.2 \pm 1.4) \times 10^{-12}$ cm³ molecule⁻¹ s⁻¹. Rate constants for reactions of CF₃CF₂CFHO₂ radicals with NO and NO₂ were $k_3 > 8 \times 10^{-12}$ and $k_4 = (6.3 \pm 0.7) \times 10^{-12}$ cm³ molecule⁻¹ s⁻¹, respectively. Using a FTIR spectrometer/smog chamber technique it was shown that, under atmospheric conditions, reaction with O₂ and decomposition via C–C bond scission are competing loss mechanisms for CF₃CF₂CFHO radicals. A lower limit of 10⁵ s⁻¹ was deduced for the rate of decomposition of CF₃CF₂CFHO radicals via C–C bond scission at 296 K in 1 bar of SF₆ diluent. It is estimated that in the atmosphere approximately 98% of CF₃CF₂CFHO radicals will undergo decomposition into C₂F₅ radicals and HC(O)F and 2% will react with O₂ to give C₂F₅C(O)F. As part of this work relative rate methods were used to measure rate constants of $(1.3 \pm 0.3) \times 10^{-12}$ and $(1.5 \pm 0.3) \times 10^{-15}$ cm³ molecule⁻¹ s⁻¹ for the reactions of CF₃CF₂CFH₂ with F and Cl atoms, respectively.

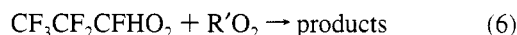
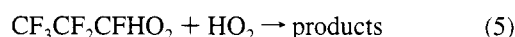
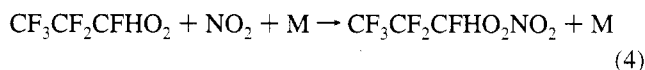
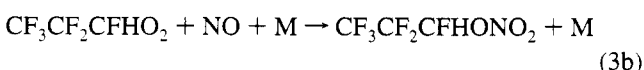
Introduction

Recognition of the adverse impact of chlorofluorocarbons, CFCs, on stratospheric ozone¹ has led to an international effort to replace CFCs with environmentally acceptable alternatives. Hydrofluorocarbons (HFCs) are one class of CFC replacements used in refrigeration and foam blowing and cleaning applications. HFC-236cb (CF₃CF₂CFH₂) has a chemical structure which is very similar to that of HFC-134a (CF₃CFH₂), which is an example of an HFC which has already found widespread use in automobile air conditioning and domestic refrigeration units.

The atmospheric chemistry of CF₃CF₂CFH₂ is of interest for two reasons. First, information concerning HFC-236cb is needed to determine the environmental impact of its release. Second, in light of its structural similarity to HFC-134a, information concerning HFC-236cb sheds light on the atmospheric chemistry of HFC-134a. The main atmospheric loss mechanism for CF₃CF₂CFH₂ is reaction with OH radicals in the lower atmosphere to produce fluorinated alkyl radicals which react rapidly with O₂ to give peroxy radicals, CF₃CF₂CFHO₂.



In the atmosphere the CF₃CF₂CFHO₂ radicals will react with NO, NO₂, HO₂, or other peroxy radicals:²

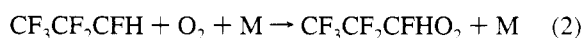
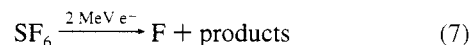


We have used a pulse radiolysis technique to determine the UV absorption spectrum of CF₃CF₂CFHO₂ and the kinetics of reactions 3, 4, and 6. The fate of the CF₃CF₂CFHO radical produced in reaction 3 was determined using a FTIR spectrometer coupled to an atmospheric reactor. The results are reported herein.

Experimental Section

The two experimental systems used have been described previously^{3,4} and are discussed briefly here.

Pulse Radiolysis System. Radicals were generated by irradiation of SF₆/O₂/CF₃CF₂CFH₂ gas mixtures in a 1 L stainless steel reaction cell with a 30 ns pulse of 2 MeV electrons from a Febetron 705B field emission accelerator. SF₆ was always in great excess and was used to generate fluorine atoms:



Transient absorptions were followed by multipassing the output of a pulsed 150 W Xenon arc lamp through the reaction cell using internal White cell optics. Total path lengths of 80 and 120 cm were used. The analyzing light was guided through

[†] Present address: Institute of Life Sciences and Chemistry, Roskilde University, P.O. Box 260, DK-4000 Roskilde, Denmark.

[®] Abstract published in *Advance ACS Abstracts*, October 15, 1995.

a 1 m McPherson grating UV-vis monochromator and detected with a Hamamatsu photomultiplier. The spectral resolution was 0.8 nm. Reagent concentrations used were as follows: SF₆, 900–950 mbar; O₂, 0–20 mbar; CF₃CF₂CFH₂, 0–40, mbar; NO, 0.22–0.71 mbar; and NO₂, 0.19–0.74 mbar. All experiments were performed at 296 K. Ultrahigh-purity O₂ was supplied by L'Air Liquide, SF₆ (99.9%) was supplied by Gerling and Holz, CF₃CF₂CFH₂ (>97%) was obtained from PCR Inc., NO (99.8%) was obtained from Messer Grieshem, and NO₂ (>98%) was obtained from Linde Technische Gase. All reagents were used as received.

Prior to the present series of experiments the F atom yield at full dose was determined. This was achieved by monitoring the transient absorbance at 260 nm due to methylperoxy radicals produced by pulse radiolysis of SF₆/CH₄/O₂ mixtures as described elsewhere.⁷ Using a value of 3.18×10^{-18} cm² molecule⁻¹ for $\sigma(\text{CH}_3\text{O}_2)$ at 260 nm,⁵ the F atom yield was determined to be $(3.02 \pm 0.31) \times 10^{15}$ cm⁻³ at full radiation dose and 1000 mbar of SF₆. The quoted error on the F atom yield includes both statistical (two standard deviations) and potential systematic errors associated with a 10% uncertainty in $\sigma(\text{CH}_3\text{O}_2)$. Unless otherwise stated, quoted uncertainties throughout this paper are two standard deviations from statistical analysis of the data; uncertainties were propagated using conventional error analysis methods.

Five sets of experiments were performed using the pulse radiolysis system. First, the kinetics of the reaction of HFC-236cb with F atoms was studied by observing the absorbance maximum following the radiolysis of SF₆/O₂/CF₃CF₂CFH₂ mixtures and varying the CF₃CF₂CFH₂ concentration. Second, the ultraviolet absorption spectrum of CF₃CF₂CFHO₂ radicals was determined by observing the maximum in the transient UV absorption at short times (0–10 μs) following the radiolysis of SF₆/O₂/CF₃CF₂CFH₂ mixtures. Third, the decay of CF₃CF₂CFHO₂ was followed at long times (up to 400 μs) to derive a value for the self-reaction rate constant. Fourth, the kinetics of the reaction with NO was determined by observing the increase in NO₂ concentration at 400 and 450 nm following the radiolysis of SF₆/O₂/CF₃CF₂CFH₂/NO mixtures. Fifth, for the reaction with NO₂ similar experiments were performed using SF₆/O₂/CF₃CF₂CFH₂/NO₂ mixtures and observing the decay in NO₂ concentration.

FTIR/Smog Chamber System. The FTIR system was interfaced to a 140 L Pyrex reactor. Radicals were generated by the UV irradiation of mixtures of 135 mTorr of CF₃CF₂CFH₂, 136 mTorr of Cl₂, and 46–700 Torr of O₂ in 700 Torr total pressure with N₂ diluent at 296 K using 22 black lamps (760 Torr = 1013 mbar). The loss of reactants and the formation of products were monitored by FTIR spectroscopy, using an analyzing path length of 26 m and a resolution of 0.25 cm⁻¹. Infrared spectra were derived from 32 co-added spectra. CF₃CF₂CFH₂, COF₂, HC(O)F, CF₃O₃C₂F₅, and C₂F₅C(O)F were monitored using their characteristic features over the wavenumber range 800–2000 cm⁻¹. With the exception of CF₃O₃C₂F₅, reference spectra were acquired by expanding known volumes of reference materials into the reactor. CF₃O₃C₂F₅ was identified and quantified using the procedure outlined by Sehested et al.⁶

Results

Kinetics of the Reaction F + CF₃CF₂CH₂F. To determine the rate constant for reaction 8, experiments were performed using mixtures of 20 mbar of O₂, 980 mbar of SF₆, and 0–30 mbar of CF₃CF₂CH₂F. Following the radiolysis pulse, reactions

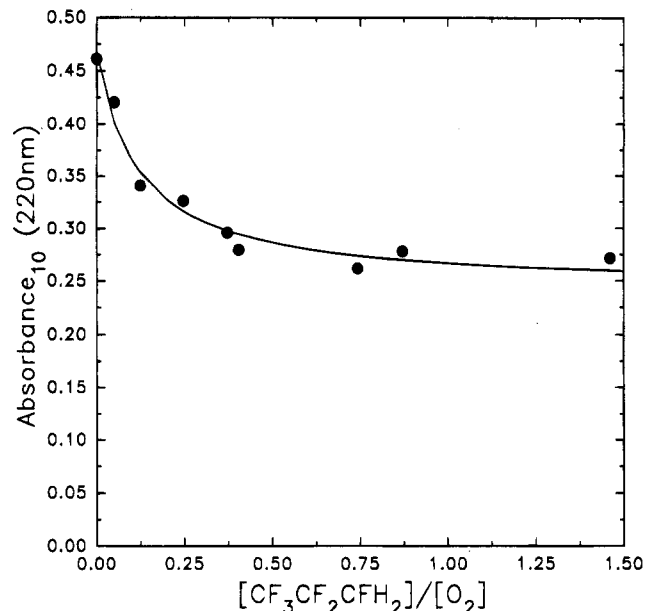
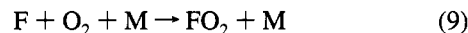


Figure 1. Plot of maximum transient absorbance as a function of the concentration ratio $[\text{CF}_3\text{CF}_2\text{CFH}_2]/[\text{O}_2]$, following the radiolysis of 0–30 mbar of CF₃CF₂CFH₂, 20 mbar of O₂, and 980 mbar of SF₆. The UV path length was 80 cm, and the radiolysis dose was 42% of maximum dose.

8 and 9 compete for the available F atoms.



CF₃CF₂CFH radicals formed in reaction 8 react with O₂ to give CF₃CF₂CFHO₂ radicals. FO₂ and CF₃CF₂CFHO₂ radicals both absorb at 220 nm. The maximum absorbance at 220 nm following the radiolysis of CF₃CF₂CFH₂/O₂/SF₆ mixtures is plotted as a function of the concentration ratio $[\text{CF}_3\text{CF}_2\text{CH}_2\text{F}]/[\text{O}_2]$ in Figure 1. The y-axis intercept in Figure 1 is the absorbance when all the F atoms are converted into FO₂ radicals. Because a given concentration of FO₂ radicals absorb more strongly than the same concentration of CF₃CF₂CFHO₂ radicals, the maximum absorbance decreases as the $[\text{CF}_3\text{CF}_2\text{CH}_2\text{F}]/[\text{O}_2]$ ratio increases. The decrease in maximum absorbance continues until the $[\text{CF}_3\text{CF}_2\text{CH}_2\text{F}]/[\text{O}_2]$ ratio is about 0.7. Further increase in the $[\text{CF}_3\text{CF}_2\text{CH}_2\text{F}]/[\text{O}_2]$ ratio does not affect the maximum absorbance. The measured maximum absorbance, A_{max} , is a function of the rate constants for reactions 8 and 9 and the expected absorbances if only FO₂ or CF₃CF₂CFHO₂ were produced, $A(\text{FO}_2)$ and $A(\text{CF}_3\text{CF}_2\text{CFHO}_2)$, as expressed in the following equation:

$$A_{\text{max}} = \{A(\text{FO}_2) + A(\text{CF}_3\text{CF}_2\text{CFHO}_2)(k_8/k_9)[\text{CF}_3\text{CF}_2\text{CH}_2\text{F}]/[\text{O}_2]\} / \{1 + (k_8/k_9)[\text{CF}_3\text{CF}_2\text{CH}_2\text{F}]/[\text{O}_2]\}$$

The rate constant ratio k_8/k_9 was calculated by performing a three-parameter fit of this expression to the data in Figure 1 in which the parameters $A(\text{FO}_2)$, $A(\text{CF}_3\text{CF}_2\text{CFHO}_2)$, and k_8/k_9 were varied simultaneously. The best fit is shown as the solid line in Figure 1 and was achieved using $k_8/k_9 = 8.2 \pm 4.6$. Using $k_9 = (1.9 \pm 0.3) \times 10^{-13}$,⁷ we find $k_8 = (1.6 \pm 0.9) \times 10^{-12}$ cm³ molecule⁻¹ s⁻¹. This result is in agreement with a value of $k_8 = (1.3 \pm 0.3) \times 10^{-12}$ cm³ molecule⁻¹ s⁻¹ measured using a relative rate technique described in a subsequent section of the present paper.

Absorption Spectrum of CF₃CF₂CFH₂O₂. Following the pulse radiolysis of mixtures of 20 mbar of O₂, 40 mbar of CF₃CF₂CFH₂, and 940 mbar of SF₆, a rapid increase in the UV absorption was observed; see Figure 2. It seems reasonable to ascribe this absorbance to the formation of the CF₃CF₂CFHO₂ radical through reactions 2, 7, and 8.

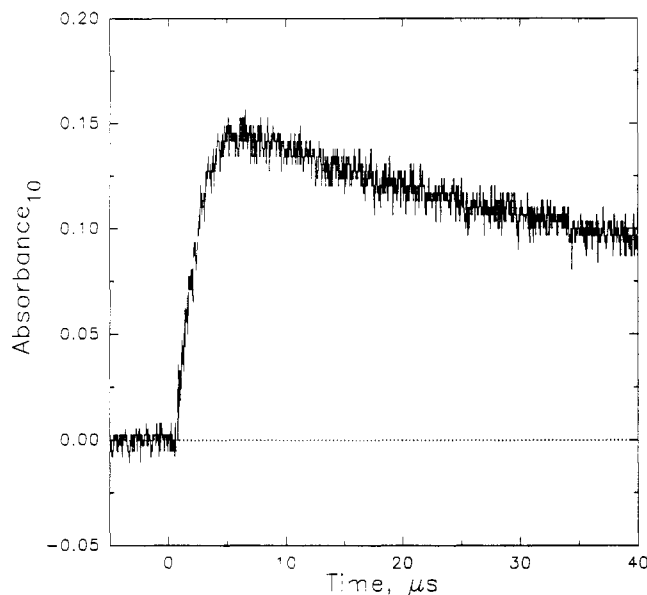
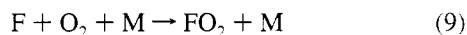
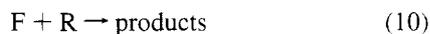


Figure 2. Transient absorption at 250 nm following the pulsed radiolysis (full dose) of a mixture of 20 mbar of O₂, 40 mbar of CF₃CF₂CFH₂, and 940 mbar of SF₆.

Before we are able to calculate the absorption cross section of the RO₂ radical, we need to consider possible complications. After the radiolysis pulse, reactions 8 and 9 compete for the available F atoms.



With experimental conditions of 20 mbar of O₂, 40 mbar of CF₃CF₂CFH₂, and 940 mbar of SF₆ and the rate constants $k_8 = 1.3 \times 10^{-12}$ (this work) and $k_9 = 1.9 \times 10^{-13} \text{ cm}^3 \text{ molecule}^{-1} \text{ s}^{-1}$ (ref 7), it can be calculated that 93.2% of the initial F atoms react with CF₃CF₂CFH₂ to give CF₃CF₂CFH (and hence CF₃CF₂CFHO₂) and 6.8% react with O₂ to give FO₂. We also need to consider unwanted radical-radical reactions such as



To check for these reactions, experiments were performed with mixtures of 20 mbar of O₂, 40 mbar of CF₃CF₂CFH₂, and 940 mbar of SF₆ with the radiolysis dose varied over an order of magnitude. In Figure 3 the maximum absorbance observed at 250 nm using a path length of 80 cm is plotted as a function of radiolysis dose.

As seen from Figure 3, the maximum transient absorbance was linear with radiolysis dose up to about 42% of the maximum dose. At higher dose the absorbance was smaller than expected from a linear extrapolation of the low dose experiments. We ascribe the curvature to incomplete conversion of F atoms to CF₃CF₂CFHO₂ caused by radical-radical reactions such as reactions 10–12. Subsequent experiments were thus performed using a radiolysis dose which was 41.6% of the maximum.

The solid line drawn through the data in Figure 3 is a linear least squares fit of the low-dose data. The slope is 0.169 ± 0.008 . From this and three additional pieces of information [(i) the F atom yield of $(3.02 \pm 0.3) \times 10^{15} \text{ molecules cm}^{-3}$ at full dose and SF₆ pressure of 1000 mbar, (ii) the conversion of F atoms into 93.2% CF₃CF₂CFHO₂ and 6.8% FO₂, and (iii) the absorption cross section of FO₂ at 250 nm ($\sigma = 130 \times 10^{-20} \text{ cm}^2 \text{ molecule}^{-1}$)],⁷ we derive $\sigma(\text{CF}_3\text{CF}_2\text{CFHO}_2) = (175 \pm 36) \times$

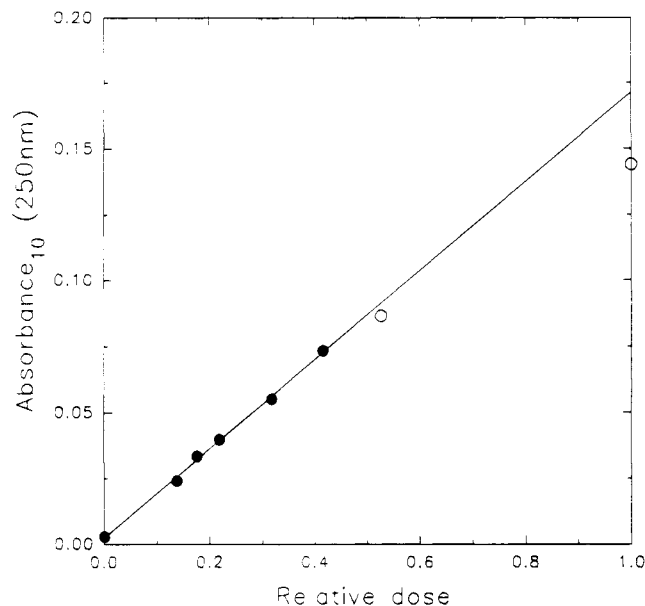


Figure 3. Maximum transient absorbance as a function of radiolysis dose at 250 nm following the pulse radiolysis of mixtures of 20 mbar of O₂, 40 mbar of CF₃CF₂CFH₂, and 940 mbar of SF₆. The UV path length was 80 cm. The line is a linear least squares fit to the low dose data (filled symbols).

TABLE 1: Measured Absorption Cross Sections

wavelength (nm)	σ ($10^{-20} \text{ cm}^2 \text{ molecule}^{-1}$)	wavelength (nm)	σ ($10^{-20} \text{ cm}^2 \text{ molecule}^{-1}$)
215	525	250	175
220	512	255	138
225	508	260	93
227	492	265	66
230	424	270	41
235	382	280	22
240	316	300	6
245	239		

$10^{-20} \text{ cm}^2 \text{ molecule}^{-1}$ at 250 nm. To map out the spectrum of CF₃CF₂CFHO₂, experiments were performed to measure the maximum transient absorbance between 215 and 300 nm following the pulsed irradiation of SF₆/CF₃CF₂CFH₂/O₂ mixtures. The observed absorbance values were scaled to that at 250 nm and corrected for FO₂ using FO₂ absorption cross sections measured by Ellermann et al.⁷ to obtain absolute absorption cross sections for CF₃CF₂CFHO₂. Absorption cross sections are given in Table 1 and shown in Figure 4. The absorption spectrum of CF₃CF₂CFHO₂ is compared to those of CF₃CF₂O₂⁶ and CF₃CFHO₂⁸ in Figure 4. The spectra of the different peroxy radicals are similar in shape. There is a tendency to a shift to the blue by substitution of F atoms with H atoms consistent with literature spectra of halogenated peroxy radicals, where substitution of increasingly electron withdrawing groups on the carbon atom bearing the O–O• group results in a shift of the spectrum toward shorter wavelengths.^{2,9} As expected for radicals of such similar structure, the spectra of CF₃CFHO₂ and CF₃CF₂CFHO₂ are indistinguishable.

CF₃CF₂CFHO₂ Self Reaction. After the rapid increase in absorbance following pulsed radiolysis of mixtures of 40 mbar of CF₃CF₂CFH₂, 20 mbar of O₂, and 960 mbar of SF₆ a slower decay of the absorbance was observed. We ascribe this decay to the self reaction of the peroxy radicals.



The kinetic expression of reaction 13 is $-d[\text{CF}_3\text{CF}_2\text{CFHO}_2]/dt = 2k_{13\text{obs}}[\text{CF}_3\text{CF}_2\text{CFHO}_2]^2$. The second-order decay expression is $A(t) = (A_0 - A_{\text{inf}})/(1 + 2k_{13\text{obs}}(A_0 - A_{\text{inf}})t) + A_{\text{inf}}$, where

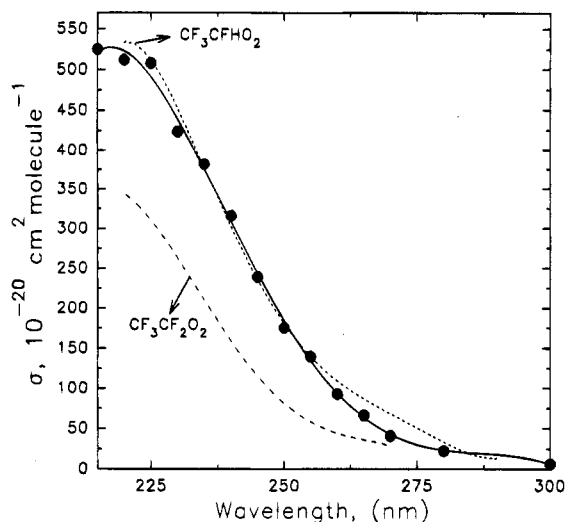


Figure 4. Absorption cross sections for $\text{CF}_3\text{CF}_2\text{CFHO}_2$ measured in this work (\bullet) compared to those for CF_3CFHO_2 (short dash)⁸ and $\text{CF}_3\text{CF}_2\text{O}_2$ (long dash).⁶ The solid line is a fifth-order regression to the $\text{CF}_3\text{CF}_2\text{CFHO}_2$ data to aid visual inspection.

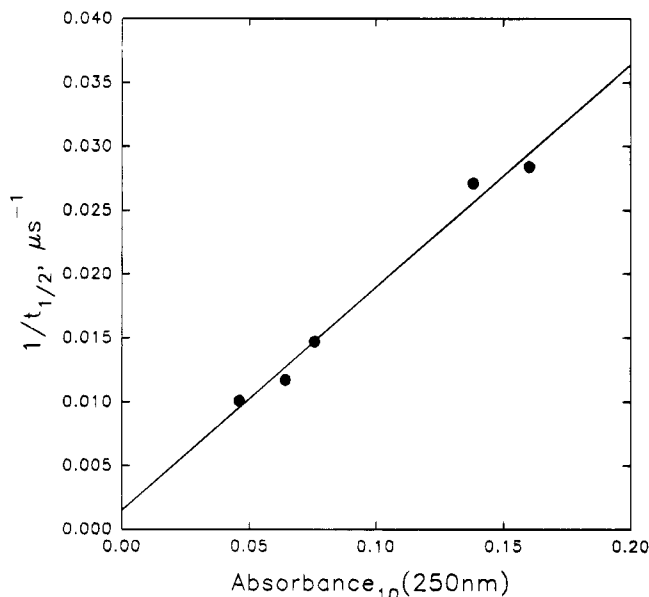


Figure 5. Plot of $1/t_{1/2}$ for the self reaction of $\text{CF}_3\text{CF}_2\text{CFHO}_2$ as a function of maximum absorbance at 250 nm.

$A(t)$ is the measured absorbance at time t , A_0 is the absorbance at time zero, A_{inf} is the absorbance at infinite time, and $k_{13\text{obs}}$ is the observed second-order rate constant. This expression was fitted to the observed decay to derive the half-life of the decay, $t_{1/2}$. In Figure 5 $1/t_{1/2} = 2k_{13\text{obs}}[\text{CF}_3\text{CF}_2\text{CFHO}_2]$ is plotted versus the maximum absorbance at 250 nm. The datapoints were obtained using different radiolysis doses. As discussed above, at 250 nm a certain fraction of the initial absorbance is attributable to the formation of FO_2 radicals in reaction 9. The data presented in Figure 5 have been corrected for FO_2 absorption. Linear least squares regression of the data in Figure 5 gives a slope of $(1.7 \pm 0.3) \times 10^5 \text{ s}^{-1} = 2k_{13\text{obs}} \ln(10)/(80 \text{ cm} \times \sigma_{250}(\text{CF}_3\text{CF}_2\text{CFHO}_2))$. Using $\sigma_{250}(\text{CF}_3\text{CF}_2\text{CFHO}_2) = (175 \pm 36) \times 10^{-20} \text{ cm}^2 \text{ molecule}^{-1}$, we obtain $k_{13\text{obs}} = (5.2 \pm 1.4) \times 10^{-12} \text{ cm}^3 \text{ molecule}^{-1} \text{ s}^{-1}$. As discussed previously,⁶ the peroxy radicals might react with products of their self reaction.^{6,10} In addition CF_3CF_2 and hence $\text{CF}_3\text{CF}_2\text{O}_2$ radicals may be formed which absorb at 250 nm, complicating the kinetic analysis. Hence, our measured $k_{13\text{obs}}$ may not be the true bimolecular rate constant for reaction 13, k_{13} . In the absence of information concerning the reactivity of the $\text{CF}_3\text{CF}_2\text{CFHO}_2$ radicals toward species formed following their self reaction (e.g.,

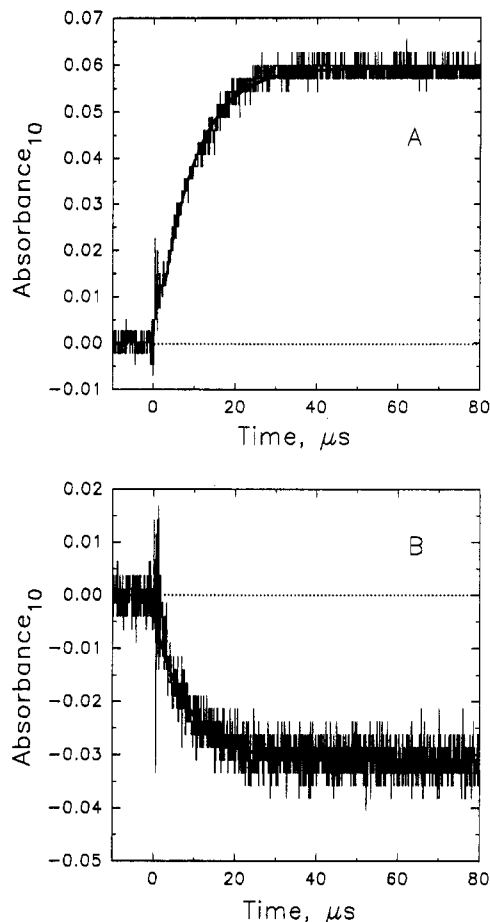


Figure 6. Transient absorbance traces at 400 nm following pulsed radiolysis of mixtures of 40 mbar of $\text{CF}_3\text{CF}_2\text{CFH}_2$, 20 mbar of O_2 , and 940 mbar of SF_6 with either 0.51 mbar of NO (A) or 0.28 mbar of NO_2 (B). The UV path length was 120 cm, and the radiolysis dose was 42% of maximum dose.

$\text{C}_2\text{F}_5\text{O}_2$ and HO_2), it is not possible at this time to calculate the necessary corrections needed to convert $k_{13\text{obs}}$ into k_{13} .

Reaction of $\text{CF}_3\text{CF}_2\text{CFHO}_2$ with NO . The kinetics of the reactions between various peroxy radicals and NO have been studied in the past using an experimental method identical to the one used in this work.¹¹ We observed an increase in absorbance at 400 nm following pulsed radiolysis of mixtures of 40 mbar of $\text{CF}_3\text{CF}_2\text{CFH}_2$, 20 mbar of O_2 , and 0.22–0.71 mbar of NO with SF_6 added to a total pressure of 1 bar. NO_2 absorbs significantly at 400 nm, and we ascribe the increase in absorbance following radiolysis of $\text{SF}_6/\text{O}_2/\text{CF}_3\text{CF}_2\text{CFH}_2/\text{NO}$ mixtures to formation of NO_2 via reaction 3.



The transient absorbances were fitted to the expression $A(t) = (A_{\infty} - A_0)[1 - \exp(-k^{\text{1st}}t)] + A_0$ with the fit starting 3 μs after the electron pulse to allow for the time taken for formation of the peroxy radical. Figure 6A shows a typical transient absorption; the smooth line is the first-order fit with $k^{\text{1st}} = 1.17 \times 10^5 \text{ s}^{-1}$. The bimolecular rate constant is obtained by plotting the pseudo-first-order rate constants from each experiment versus $[\text{NO}]_0$ and performing a linear least squares analysis. As seen in Figure 7 the linear fit yields $k_3 = (7.7 \pm 0.2) \times 10^{-12} \text{ cm}^3 \text{ molecule}^{-1} \text{ s}^{-1}$. The y-axis intercept $(0.9 \pm 0.6) \times 10^4 \text{ s}^{-1}$ is significantly different from zero. This intercept is caused by unwanted reactions such as the self reaction of the peroxy radical. To assess the impact of such reactions, the chemical system was simulated using the computer modeling program CHEMSIMUL.¹² A detailed calculation of each data

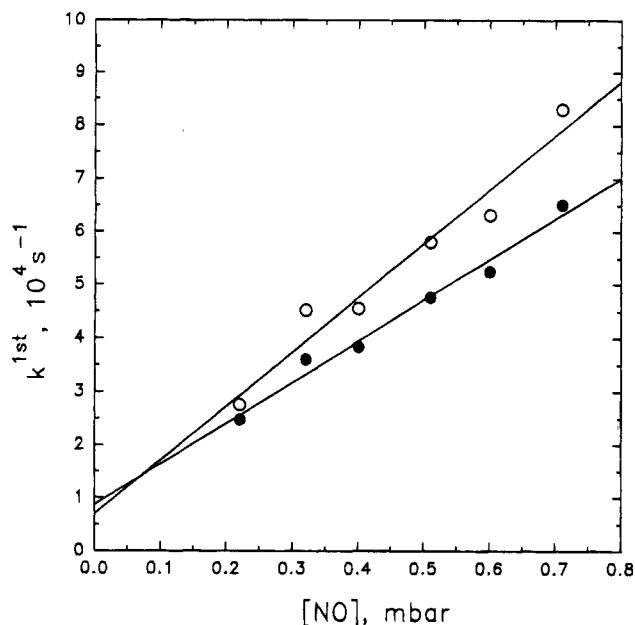


Figure 7. Plot of k^{1st} versus $[NO]$. Filled circles are observed values for k^{1st} , and open circles are corrected data; see text for details.

point was made with a mechanism consisting of reactions 2, 4, 8, 9, and 13 with $k_2 = 1.0 \times 10^{-12}$, $k_4 = 6.3 \times 10^{-12}$, $k_{13} = 5.2 \times 10^{-12}$, $k_8 = 1.3 \times 10^{-12}$, and $k_9 = 1.9 \times 10^{-13}$ $\text{cm}^3 \text{ molecule}^{-1} \text{ s}^{-1}$. Reactions of NO with F atoms and $\text{CF}_3\text{CF}_2\text{-CFH}$ and $\text{CF}_3\text{CF}_2\text{CFHO}$ radicals and reactions of NO_2 with F atoms and $\text{CF}_3\text{CF}_2\text{CFHO}$ radicals were also included. The following rate constants were used: $k_{\text{F+NO}} = 5.1 \times 10^{-12}$ (average from refs 13 and 14), $k_{\text{R+NO}} = 5.0 \times 10^{-12}$, $k_{\text{RO+NO}} = 1.0 \times 10^{-11}$, $k_{\text{RO+NO}_2} = 1.0 \times 10^{-11}$, and $k_{\text{F+NO}_2} = 1.0 \times 10^{-11}$ $\text{cm}^3 \text{ molecule}^{-1} \text{ s}^{-1}$.¹⁵

A first-order fit was made to the simulated results. In all cases the simulated data obeyed first-order kinetics. Corrections for the influence of secondary chemistry were computed and were in the range 11–28%. The main reason for these corrections is that the formation rate of RO_2 radicals is comparable to the formation rate of NO_2 . This complication slows down the formation rate of NO_2 compared to what it would be if the formation of RO_2 radicals was instantaneous. The corrected data are shown in Figure 7. Linear least squares analysis of the corrected data gives $k_3 = (1.02 \pm 0.22) \times 10^{-11}$ $\text{cm}^3 \text{ molecule}^{-1} \text{ s}^{-1}$ and a y-axis intercept of $(0.7 \pm 1.1) \times 10^4$ s^{-1} , which is not statistically significant.

The NO_2 yield expressed in terms of moles of NO_2 formed per mole of F atoms consumed was $163 \pm 13\%$. Corrections were made for the consumption of F atoms by reaction with O_2 and NO. The fact that the NO_2 yield is greater than 100% can be explained by formation of NO_2 via the reactions of NO with decomposition products of the alkoxy radical $\text{CF}_3\text{CF}_2\text{CFHO}$ (see subsequent section). The formation of NO_2 from reactions occurring subsequent to reaction 3 introduces a delay in the overall NO_2 formation profile. Thus, the rate constant $k_3 = (1.02 \pm 0.22) \times 10^{-11}$ $\text{cm}^3 \text{ molecule}^{-1} \text{ s}^{-1}$ determined in the present work should be regarded as a lower limit for the rate constant for reaction 3. Hence, $k_3 > 8 \times 10^{-12}$ $\text{cm}^3 \text{ molecule}^{-1} \text{ s}^{-1}$. This result can be compared to rate constants for reactions of peroxy radicals derived from reactions of other HFCs with NO. For $\text{CF}_3\text{CH}_2\text{O}_2$, $k = (1.2 \pm 0.3) \times 10^{-11}$ $\text{cm}^3 \text{ molecule}^{-1} \text{ s}^{-1}$,⁹ and for CF_3CFHO_2 , $k = (1.31 \pm 0.41) \times 10^{-11}$ $\text{cm}^3 \text{ molecule}^{-1} \text{ s}^{-1}$.⁸ These values are consistent with the rate constant measured in this study.

In a subsequent section dealing with the atmospheric fate of $\text{CF}_3\text{CF}_2\text{CFHO}$ radicals, we show that for the experimental

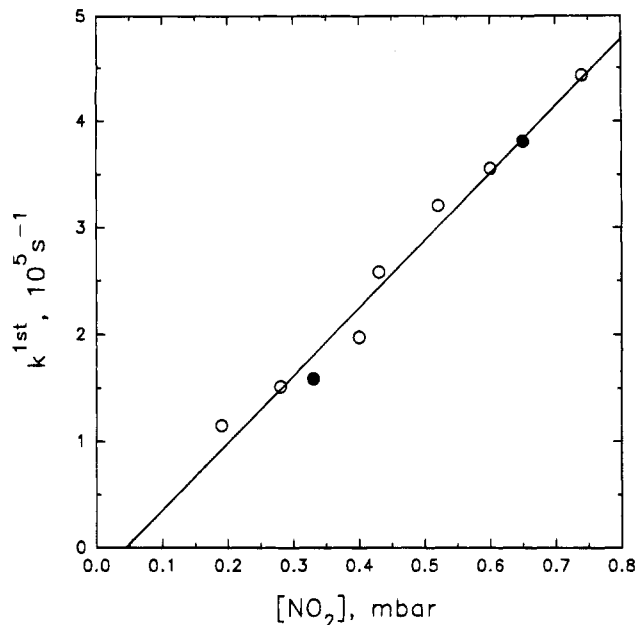
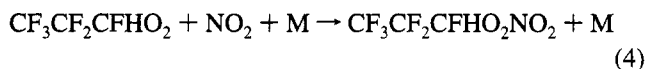
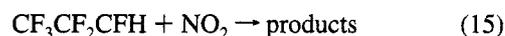


Figure 8. Plot of k^{1st} versus $[\text{NO}_2]$. Open circles are data points obtained at 400 nm, and filled circles are points obtained at 450 nm.

conditions of the above experiments (20 mbar of O_2) 99.8% of the $\text{CF}_3\text{CF}_2\text{CFHO}$ will undergo decomposition while 0.2% will react with O_2 . The fact that the NO_2 yield is substantially greater than 100% is therefore due to the rapid decomposition of $\text{CF}_3\text{-CF}_2\text{CFHO}$ radicals. Detailed simulations of experimental traces such as that shown in Figure 6A place an upper limit of 10 μs on the lifetime of $\text{CF}_3\text{CF}_2\text{CFHO}$ radicals in the system. Hence, the rate of decomposition of $\text{CF}_3\text{CF}_2\text{CFHO}$ radicals must be faster than 10^5 s^{-1} .

Reaction of $\text{CF}_3\text{CF}_2\text{CFHO}_2$ with NO_2 . The reaction between $\text{CF}_3\text{CF}_2\text{CFHO}_2$ radicals and NO_2 was investigated by monitoring the decay in absorbance at 400 and 450 nm following pulsed radiolysis of mixtures of 40 mbar of $\text{CF}_3\text{CF}_2\text{CFH}_2$, 20 mbar of O_2 , 0.19–0.74 mbar of NO_2 , and 940 mbar of SF_6 . Figure 6B shows the transient absorption observed in an experiment using 0.28 mbar of NO_2 . NO_2 absorbs at 400 and 450 nm; hence, the decay in absorption observed following radiolysis of $\text{SF}_6/\text{O}_2/\text{CF}_3\text{CF}_2\text{CFH}_2/\text{NO}_2$ mixtures can be ascribed to loss of NO_2 . Under the given experimental conditions, three reactions can be responsible for the loss of NO_2 :



Using $k_8 = 1.6 \times 10^{-12}$ $\text{cm}^3 \text{ molecule}^{-1} \text{ s}^{-1}$, it follows that in the presence of 40 mbar of HFC-236cb the lifetime of F atoms is 0.6 μs . Assuming a value of $k_2 = 2.0 \times 10^{-12}$ $\text{cm}^3 \text{ molecule}^{-1} \text{ s}^{-1}$ (typical for such a reaction²), the lifetime of $\text{CF}_3\text{CF}_2\text{CFH}$ radicals with respect to reaction 2 is 1.0 μs . By fitting the transient absorption shown in Figure 6B from 3 μs after the radiolysis pulse, kinetic data for reaction 4 can be obtained free from complications caused by reactions 14 and 15. Pseudo-first-order rate constants obtained are plotted as a function of $[\text{NO}_2]$ in Figure 8. The smooth line in Figure 8 is a linear least squares regression which gives $k_4 = (6.3 \pm 0.7) \times 10^{-12}$ $\text{cm}^3 \text{ molecule}^{-1} \text{ s}^{-1}$; the small negative y-axis intercept is not statistically significant. The value of k_4 measured here is entirely consistent with the high-pressure limiting rate constants for reactions between other halogenated peroxy

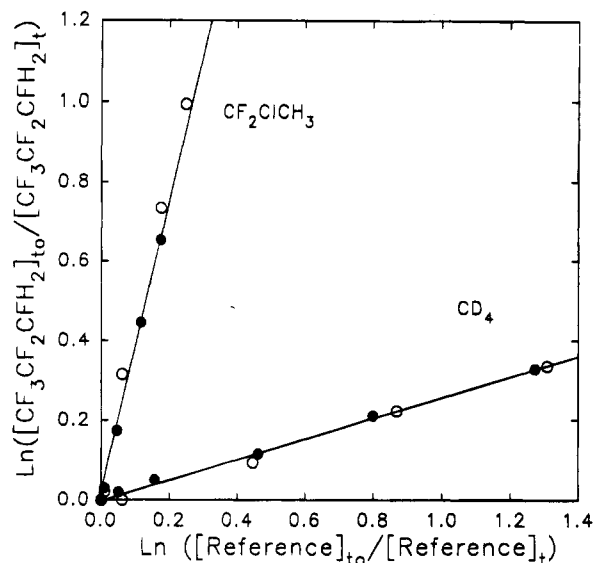
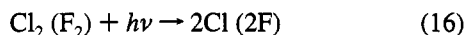


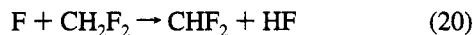
Figure 9. Loss of $\text{CF}_3\text{CF}_2\text{CFH}_2$ versus CF_2ClCH_3 and CD_4 when $\text{CF}_3\text{CF}_2\text{CFH}_2/\text{CF}_2\text{ClCH}_3$ and $\text{CF}_3\text{CF}_2\text{CFH}_2/\text{CD}_4$ mixtures were exposed to Cl atoms. Experiments were performed at 296 K in 700 Torr of either N_2 (open symbols) or air (filled symbols) diluent.

radicals and NO_2 , which lie in the range $(4.5\text{--}8.9) \times 10^{-12} \text{ cm}^3 \text{ molecule}^{-1} \text{ s}^{-1}$.^{2,9,15}

Kinetics of the Reactions of F and Cl Atoms with $\text{CF}_3\text{CF}_2\text{CFH}_2$. Before the products arising from the Cl atom initiated oxidation of $\text{CF}_3\text{CF}_2\text{CFH}_2$ were investigated, a series of relative rate experiments were performed using the FTIR setup to investigate the kinetics of the reactions of F and Cl atoms with $\text{CF}_3\text{CF}_2\text{CFH}_2$. The relative rate technique is described in detail elsewhere.^{16,17} Photolysis of the molecular halogen was used as a source of Cl or F atoms.



The kinetics of reaction 17 were measured relative to those of reactions 18 and 19. The kinetics of reaction 8 were measured relative to those of reactions 20 and 21.



The observed loss of $\text{CF}_3\text{CF}_2\text{CFH}_2$ versus those of CF_2ClCH_3 and CD_4 following the UV irradiation of $\text{CF}_3\text{CF}_2\text{CFH}_2/\text{CF}_2\text{ClCH}_3/\text{Cl}_2$ and $\text{CF}_3\text{CF}_2\text{CFH}_2/\text{CD}_4/\text{Cl}_2$ mixtures in 700 Torr total pressure of N_2 or air diluent are shown in Figure 9. Linear least squares analysis of the data in Figure 9 gives $k_{17}/k_{18} = 3.65 \pm 0.26$ and $k_{17}/k_{19} = 0.25 \pm 0.02$. Using $k_{18} = 3.8 \times 10^{-16}$ (average from refs 16 and 18) and $k_{19} = 6.1 \times 10^{-15} \text{ cm}^3 \text{ molecule}^{-1} \text{ s}^{-1}$ gives $k_{17} = (1.4 \pm 0.1) \times 10^{-15}$ and $(1.5 \pm 0.1) \times 10^{-15} \text{ cm}^3 \text{ molecule}^{-1} \text{ s}^{-1}$, respectively. We estimate that potential systematic errors associated with uncertainties in the reference rate constants could add an additional 15% to the uncertainty range. Propagating this additional 15% uncertainty together with statistical uncertainties which cover the extremes of the two determinations gives $k_{17} = (1.5 \pm 0.3) \times 10^{-15} \text{ cm}^3 \text{ molecule}^{-1} \text{ s}^{-1}$.

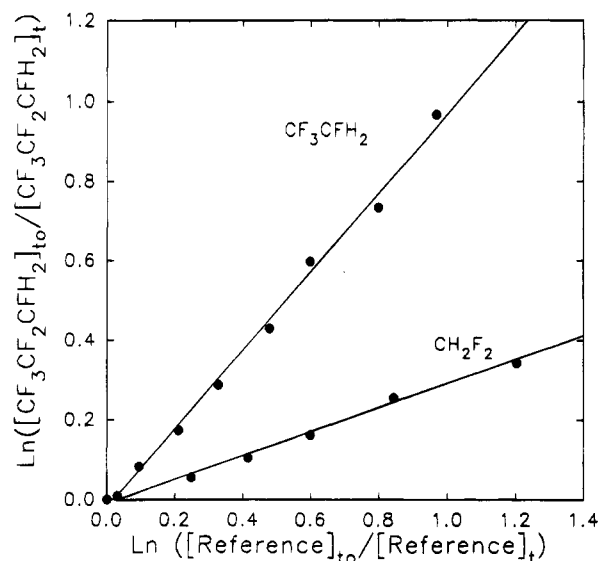


Figure 10. Loss of $\text{CF}_3\text{CF}_2\text{CFH}_2$ versus CF_3CFH_2 and CH_2F_2 when $\text{CF}_3\text{CF}_2\text{CFH}_2/\text{CF}_3\text{CFH}_2$ and $\text{CF}_3\text{CF}_2\text{CFH}_2/\text{CH}_2\text{F}_2$ mixtures were exposed to F atoms. Experiments were performed at 296 K in 700 Torr of N_2 diluent.

Figure 10 shows the observed decay of $\text{CF}_3\text{CF}_2\text{CFH}_2$, CH_2F_2 , and CF_3CFH_2 when mixtures of these compounds were exposed to F atoms in 700 Torr of air diluent. From the data in Figure 10 rate constant ratios of $k_8/k_{20} = (0.30 \pm 0.03)$ and $k_7/k_{21} = (0.99 \pm 0.08)$ are derived. The reactivities of both CH_2F_2 and CF_3CFH_2 toward F atoms have been determined previously.¹⁷ Using $k_{20} = 4.3 \times 10^{-12}$ and $k_{21} = 1.3 \times 10^{-12}$ gives identical values of $(1.3 \pm 0.1) \times 10^{-12} \text{ cm}^3 \text{ molecule}^{-1} \text{ s}^{-1}$ for k_8 . We estimate that potential systematic errors associated with uncertainties in the reference rate constants could add an additional 20% to the uncertainty range. Propagating this additional uncertainty gives $k_8 = (1.3 \pm 0.3) \times 10^{-12} \text{ cm}^3 \text{ molecule}^{-1} \text{ s}^{-1}$. This result is consistent with the value of $k_8 = (1.6 \pm 0.9) \times 10^{-12} \text{ cm}^3 \text{ molecule}^{-1} \text{ s}^{-1}$ measured using the pulse radiolysis technique as described above.

It is interesting to compare the reactivity of Cl and F atoms toward $\text{CF}_3\text{CF}_2\text{CFH}_2$ and CF_3CFH_2 . As might be anticipated for two compounds possessing such a similar chemical structure, the rate constants for reactions of F and Cl atoms with $\text{CF}_3\text{CF}_2\text{CFH}_2$ are indistinguishable from those of the corresponding reactions involving CF_3CFH_2 .^{16,17}

Study of the Atmospheric Fate of $\text{CF}_3\text{CF}_2\text{CFHO}$ Radicals. To determine the atmospheric fate of the alkoxy radical $\text{CF}_3\text{CF}_2\text{CFHO}$ formed in reaction 3, two sets of experiments were performed in which $\text{Cl}_2/\text{CF}_3\text{CF}_2\text{CFH}_2/\text{O}_2$ mixtures at a total pressure of 700 Torr made up with N_2 diluent were irradiated in the FTIR/smog chamber system. The initial conditions were 135 mTorr of HFC-236cb, 136 mTorr of Cl_2 , and 46 or 700 Torr of O_2 in 700 Torr total pressure of N_2 diluent. The loss of HFC-236cb and the formation of products were monitored by FTIR spectroscopy. Four products were observed: COF_2 , HC(O)F , $\text{CF}_3\text{O}_3\text{C}_2\text{F}_5$, and $\text{C}_2\text{F}_5\text{C(O)F}$. The yields of these products are shown plotted against the loss of HFC-236cb in Figure 11. At this point it is appropriate to consider possible losses of these products in the smog chamber system. During the past 2–3 years we have gained extensive experience on the behavior of COF_2 , HC(O)F , and $\text{CF}_3\text{O}_3\text{C}_2\text{F}_5$ in the chamber; none of these compounds are lost by photolysis or heterogeneous processes and all but HC(O)F are unreactive toward Cl atoms.^{6,19} Cl atoms react with HC(O)F with a rate constant of $2.0 \times 10^{-15} \text{ cm}^3 \text{ molecule}^{-1} \text{ s}^{-1}$;¹⁹ i.e., 1.3 times more rapidly than with HFC-236cb. Corrections for the loss of HC(O)F via Cl atom attack were in the range 3–24% and have been applied to the

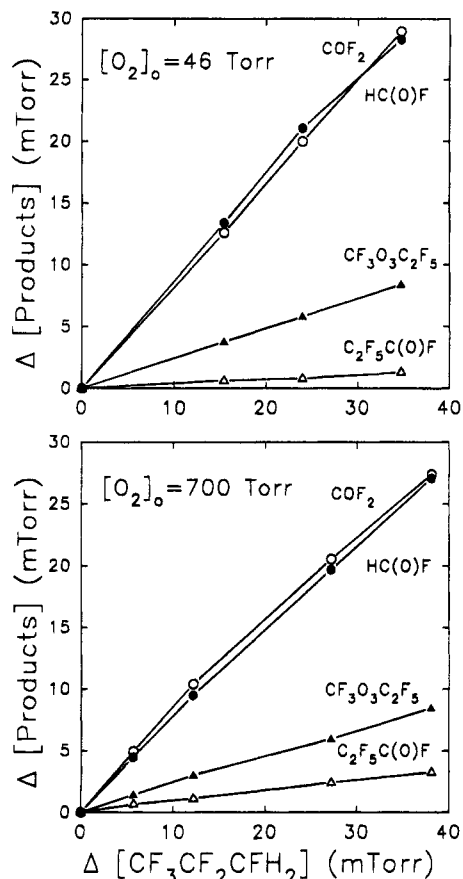
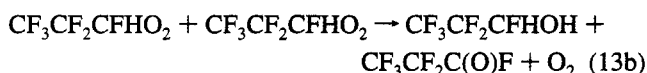


Figure 11. Formation of COF_2 (○), HC(O)F (●), $\text{CF}_3\text{O}_3\text{C}_2\text{F}_5$ (▲), and $\text{C}_2\text{F}_5\text{C(O)F}$ (△), versus loss of HFC-236cb following the UV irradiation of mixtures of 135 mTorr of $\text{CF}_3\text{CF}_2\text{CFH}_2$, 136 mTorr of Cl_2 , and either 46 (top panel) or 700 Torr (bottom panel) of O_2 in 700 Torr total pressure using N_2 diluent at 296 K.

data shown in Figure 11. The behavior of $\text{C}_2\text{F}_5\text{C(O)F}$ in the chamber has not been studied previously, and so experiments were performed to assess its possible heterogeneous loss by letting mixtures of 15 mTorr of $\text{C}_2\text{F}_5\text{C(O)F}$ and 100 mTorr of Cl_2 in 700 Torr of air stand in the chamber for 15 min; there was no discernible loss (<2%) of $\text{C}_2\text{F}_5\text{C(O)F}$. There was no loss of $\text{C}_2\text{F}_5\text{C(O)F}$ when the same mixture was subject to UV irradiation for 15 min, suggesting that $\text{C}_2\text{F}_5\text{C(O)F}$ is not lost via photolysis or reaction with Cl atoms. The average carbon balance for the three experiments performed with 46 Torr of O_2 was 84% while that for the four experiments using 700 Torr of O_2 was 85%. The shortfall of approximately 15% in the carbon balance may reflect uncertainties in the calibrations of the reference spectra or the presence of some undetected product, or both.

Following formation in the chamber via reactions 2 and 17, $\text{CF}_3\text{CF}_2\text{CFHO}_2$ radicals are expected to undergo self reaction. The alkoxy radical $\text{CF}_3\text{CF}_2\text{CFHO}$ formed in reaction (13a) will either decompose via C–C bond scission or react with O_2 .



The goal of the FTIR/smog chamber experiments was to quantify the relative importance of reactions 22 and 23 in the

atmospheric chemistry of $\text{CF}_3\text{CF}_2\text{CFHO}$ radicals. The yield of HC(O)F following irradiation of $\text{Cl}_2/\text{CF}_3\text{CF}_2\text{CFH}_2/\text{O}_2$ mixtures provides a marker for reaction 22 whereas the yield of $\text{C}_2\text{F}_5\text{C(O)F}$ is a marker for reaction 23. Examination of Figure 11 shows that HC(O)F is a major product observed in both experiments while $\text{C}_2\text{F}_5\text{C(O)F}$ is of minor importance. Hence, it can be concluded that under the present experimental conditions reaction 22 dominates reaction 23.

Let us now consider the other products observed and their dependence on the O_2 partial pressure. We have shown previously that C_2F_5 radicals formed in reaction 22 give rise to COF_2 , $\text{CF}_3\text{O}_3\text{C}_2\text{F}_5$, CF_3OH , and $\text{CF}_3\text{O}_3\text{CF}_3$ products within the chamber.⁶ As seen from Figure 11, with increased O_2 partial pressure the yields of COF_2 and HC(O)F decreased while the $\text{C}_2\text{F}_5\text{C(O)F}$ yield increased. Such behavior is consistent with a competition between reactions 22 and 23 for the available $\text{CF}_3\text{CF}_2\text{CFHO}$ radicals. The average $\text{C}_2\text{F}_5\text{C(O)F}$ and HC(O)F yields computed from the individual data points in Figure 11 are $3 \pm 1\%$ and $86 \pm 4\%$, and $9 \pm 1\%$ and $75 \pm 4\%$ for experiments with 46 and 700 Torr partial pressure of O_2 , respectively. The quoted uncertainties encompass the range of individual determinations. Assuming that $\text{C}_2\text{F}_5\text{C(O)F}$ is formed in the chamber solely by reactions 13b and 23, then its yield can be expressed as a function of the rate constant ratio k_{23}/k_{22} :¹⁹

$$\text{C}_2\text{F}_5\text{C(O)F yield} = Y_0 + (1 - 2Y_0) \left\{ \frac{(k_{23}/k_{22})[\text{O}_2]}{1 + (k_{23}/k_{22})[\text{O}_2]} \right\}$$

where Y_0 is the $\text{C}_2\text{F}_5\text{C(O)F}$ yield from reaction 13. Using the observed yields of $\text{C}_2\text{F}_5\text{C(O)F}$, we derive $k_{23}/k_{22} = (3 \pm 1) \times 10^{-21} \text{ cm}^3 \text{ molecule}^{-1}$ and $Y_0 = 0.03 \pm 0.01$. This can be compared to the analogous HFC-134a result of $k_{\text{O}_2}/k_{\text{diss}} = 5.1 \times 10^{-20} \text{ cm}^3 \text{ molecule}^{-1}$ (at 296 K and 700 Torr total pressure). Relative to the reaction with O_2 , decomposition of the alkoxy radical is approximately 17 times more important for the alkoxy radical derived from HFC-236cb than it is for the corresponding radical from HFC-134a.

Implications for Atmospheric Chemistry

The atmospheric lifetime of HFC-236cb will be determined by reaction with OH radicals. To the best of our knowledge there are no data available for the kinetics of the reaction of OH radicals with HFC-236cb. In the present work it has been shown that Cl and F atoms react with HFC-236cb at rates which are indistinguishable from their rates of reaction with HFC-134a. It seems reasonable to expect that OH radicals will react at the same rate with HFC-236cb as with HFC-134a. The atmospheric lifetime of HFC-134a is approximately 15 years, and we expect that HFC-236cb will also have a lifetime of 15 years. Reaction of OH radicals with HFC-236cb in air gives $\text{CF}_3\text{CF}_2\text{CFHO}_2$ radicals. In the present work it has been shown that $\text{CF}_3\text{CF}_2\text{CFHO}_2$ radicals react with NO to give NO_2 and, by inference, $\text{CF}_3\text{CF}_2\text{CFHO}$ radicals. Using $k_3 > 8 \times 10^{-12} \text{ cm}^3 \text{ molecule}^{-1} \text{ s}^{-1}$ and an average tropospheric NO concentration of $2.5 \times 10^8 \text{ cm}^{-3}$ ²⁰ gives a lifetime of <9 min for $\text{CF}_3\text{CF}_2\text{CFHO}_2$ radicals with respect to reaction with NO. The alkoxy radical formed has been shown to undergo both C–C bond scission and reaction with O_2 . At 296 K and 700 Torr total pressure $k_{23}/k_{22} = 3 \times 10^{-21} \text{ cm}^3 \text{ molecule}^{-1}$; hence, in 700 Torr of air decomposition accounts for 98.6% of the loss of $\text{CF}_3\text{CF}_2\text{CFHO}$ radicals. The remaining 1.4% react with O_2 . As discussed previously for the analogous alkoxy radical derived from HFC-134a,¹⁹ the relative importance of decomposition and reaction with O_2 as fates of the $\text{CF}_3\text{CF}_2\text{CFHO}$ radicals is dependent on three parameters; O_2 partial pressure, total pressure, and temperature. For a complete understanding of the atmospheric fate of $\text{CF}_3\text{CF}_2\text{CFHO}$ radicals, the dependence

of the rate constant ratio k_{23}/k_{22} on these three parameters needs to be measured over atmospherically relevant ranges. Such a study is beyond the scope of the present work. However an estimation of the relative importance of reactions 22 and 23 in the atmospheric chemistry of $\text{CF}_3\text{CF}_2\text{CFHO}$ radicals can be made by comparison with the available database for the corresponding alkoxy radical derived from HFC-134a. Experimental studies of the atmospheric fate of CF_3CFHO radicals have established that the kinetics of C–C scission are in the falloff region between second- and first-order kinetics at pressures below 700 Torr¹⁹ and that the rate constant ratio $k(\text{C–C scission})/k(\text{O}_2 \text{ reaction})$ has an effective activation energy of 7 kcal mol⁻¹.^{19,21,22} In the present work we find that, relative to the reaction with O_2 , decomposition is 17 times more rapid for the alkoxy radical derived from HFC-236cb than for that derived from HFC-134a. Assuming that the ratios of pre-exponential Arrhenius A factors for the C–C scission and O_2 reactions are the same for the two alkoxy radicals, then the factor of 17 implies that the effective activation energy for $k(\text{C–C scission})/k(\text{O}_2 \text{ reaction})$ is reduced by 1.7 kcal mol⁻¹. Thus, we derive $k_{23}/k_{22} = 1.6 \times 10^{-25} \exp(2800/T) \text{ cm}^3 \text{ molecule}^{-1}$. $\text{CF}_3\text{CF}_2\text{CFHO}$ radicals can be viewed as CF_3CFHO radicals with one F atom substituted by a CF_3 group. This substitution is likely to have a far greater impact on the rate of C–C bond scission than on H atom abstraction by O_2 . Hence, the change of 1.7 kcal mol⁻¹ should be viewed as a weakening of the C–C bond rather than a strengthening of the C–H bond in $\text{CF}_3\text{CF}_2\text{CFHO}$ compared to CF_3CFHO radicals. The expression $k_{23}/k_{22} = 1.6 \times 10^{-25} \exp(2800/T) \text{ cm}^3 \text{ molecule}^{-1}$ can be used to evaluate the overall importance of reactions 22 and 23 in the atmospheric chemistry of $\text{CF}_3\text{CF}_2\text{CFHO}$ radicals. Making the following assumptions (i) HFC-236cb is well mixed in the atmosphere and hence its concentration scales with the atmospheric density, (ii) HFC-236cb oxidation is initiated by OH radical attack at the same rate as HFC-134a oxidation, and (iii) the pressure dependence of the decomposition of $\text{CF}_3\text{CF}_2\text{CFHO}$ is the same as that for CF_3CFHO ,¹⁹ and taking the vertical profiles for OH radicals, atmospheric density, and temperature from Brasseur and Solomon²³ we calculate that 98% of the $\text{CF}_3\text{CF}_2\text{CFHO}$ radicals formed in the atmospheric oxidation of HFC-236cb will undergo decomposition and 2% will react with O_2 . As discussed elsewhere,²⁴ C_2F_5 radicals will undergo a series of reactions in the atmosphere to give COF_2 and CF_3OH , which will be incorporated into rain–cloud–sea water and hydrolyzed to give HF and CO_2 . There is no known adverse environmental impact associated with the formation of C_2F_5 radicals in the atmosphere. By analogy to the behavior of $\text{CF}_3\text{C}(\text{O})\text{F}$,²⁴ it is expected that $\text{C}_2\text{F}_5\text{C}(\text{O})\text{F}$ will not undergo any gas phase reactions and will be incorporated into rain–cloud–sea water, where hydrolysis will give $\text{C}_2\text{F}_5\text{COOH}$, which will be rained out. While the environmental impact of $\text{C}_2\text{F}_5\text{COOH}$ is unclear, its behavior is expected to be similar to that of CF_3COOH .²⁴ Given the extremely low concentrations of $\text{C}_2\text{F}_5\text{COOH}$ expected from the atmospheric degradation of HFC-236cb, the formation of $\text{C}_2\text{F}_5\text{COOH}$ is expected to be of no environmental concern.

To conclude, the present work represents the first study of

the atmospheric degradation of HFC-236cb. As expected, the behavior of HFC-236cb is very similar to that of HFC-134a. The spectra of the peroxy radicals generated from both HFCs and the reactivities of both HFCs toward F and Cl atoms are indistinguishable. Also the reactivities of the peroxy radicals toward NO and NO_2 are indistinguishable. Interestingly, the observed product data suggest that the alkoxy radical derived from HFC-236cb decomposes approximately 17 times more rapidly than that derived from HFC-134a. This finding demonstrates the sensitivity of alkoxy radical decomposition rates to small changes in the molecular configuration. From the viewpoint of assessing the environmental acceptability of HFC-236cb as a CFC replacement, the results presented herein demonstrate that the products of the atmospheric degradation of HFC-236cb are not expected to be of any environmental concern.

References and Notes

- (1) Scientific Assessment of stratospheric Ozone. Alternative Fluorocarbon Environmental Acceptability Study, World Meteorological Organization Global Ozone Research and Monitoring Project, Report No. 20; World Meteorological Organization: Geneva, 1989; Vols. I and II.
- (2) Lightfoot, P. D.; Cox, R. A.; Crowley, J. N.; Destriau, M.; Hayman, G. D.; Jenkin, K. E.; Moortgat, G. K.; Zabel, F. *Atmos. Environ.* **1992**, *26A*, 1805.
- (3) Wallington, T. J.; Japar, S. M. *J. Atmos. Chem.* **1989**, *9*, 399.
- (4) Nielsen, O. J. Risø-R-480, 1984.
- (5) Wallington, T. J.; Dagaut, P.; Kurylo, M. J. *Chem. Rev.* **1992**, *92*, 667.
- (6) Sehested, J.; Ellermann, T.; Nielsen, O. J.; Wallington, T. J.; Hurley, M. D. *Int. J. Chem. Kinet.* **1993**, *25*, 701.
- (7) Ellermann, T.; Sehested, J.; Nielsen, O. J.; Pagsberg, P.; Wallington, T. J. *Chem. Phys. Lett.* **1994**, *218*, 287.
- (8) Wallington, T. J.; Nielsen, O. J. *Chem. Phys. Lett.* **1991**, *187*, 33.
- (9) Nielsen, O. J.; Gamborg, E.; Sehested, J.; Wallington, T. J.; Hurley, M. D. *J. Phys. Chem.* **1994**, *98*, 9518.
- (10) Nielsen, O. J.; Ellermann, T.; Sehested, J.; Bartkiewicz, E.; Wallington, T. J.; Hurley, M. D. *Int. J. Chem. Kinet.* **1992**, *24*, 1009.
- (11) Sehested, J.; Nielsen, O. J.; Wallington, T. J. *Chem. Phys. Lett.* **1993**, *213*, 457.
- (12) Rasmussen, O. L.; Bjergbakke, E. B. Risø-R-395, 1984.
- (13) Sehested, J. *Int. J. Chem. Kinet.* **1994**, *26*, 1023.
- (14) Wallington, T. J.; Ellermann, T.; Nielsen, O. J.; Sehested, J. *J. Phys. Chem.* **1994**, *98*, 2346.
- (15) Møgelberg, T. E.; Nielsen, O. J.; Sehested, J.; Wallington, T. J.; Hurley, M. D. *J. Phys. Chem.* **1995**, *99*, 1995.
- (16) Wallington, T. J.; Hurley, M. D. *Chem. Phys. Lett.* **1992**, *189*, 437.
- (17) Wallington, T. J.; Hurley, M. D.; Shi, J.; Maricq, M. M.; Sehested, J.; Nielsen, O. J.; Ellermann, T. *Int. J. Chem. Kinet.* **1993**, *25*, 651.
- (18) Tuazon, E. C.; Atkinson, R.; Corchnoy, S. B. *Int. J. Chem. Kinet.* **1992**, *24*, 639.
- (19) Wallington, T. J.; Hurley, M. D.; Ball, J. C.; Kaiser, E. W. *Environ. Sci. Technol.* **1992**, *26*, 1318.
- (20) Atkinson, R. Scientific Assessment of Stratospheric Ozone. World Meteorological Organization Global Ozone Research and Monitoring Project, Report No. 20; World Meteorological Organization, Geneva, 1989; Vol. II, p 167.
- (21) Tuazon, E. C.; Atkinson, R. *J. Atmos. Chem.* **1993**, *16*, 301.
- (22) Rattigan, O. V.; Rowley, D. M.; Wild, O.; Jones, R. L.; Cox, R. A. *J. Chem. Soc. Faraday Trans.* **1994**, *90*, 1819.
- (23) Brasseur, G.; Solomon, S. *Aeronomy of the Middle Atmosphere*; Reidel: Dordrecht, 1986.
- (24) Wallington, T. J.; Worsnop, D. R.; Nielsen, O. J.; Sehested, J.; DeBruyn, W.; Shorter, J. A. *Environ. Sci. Technol.* **1994**, *28*, 320A.

JP951744F